ELSEVIER

Polymer 43 (2002) 6287–6293

polymer

www.elsevier.com/locate/polymer

Time-resolved optical spectroscopy study of the local dynamics of *cis*-1,4 and vinyl-1,2-polybutadiene in dilute solution at high pressure

B.J. Punchard, A. Kirpatch, D.B. Adolf*

Department of Physics and Astronomy, University of Leeds, Leeds LS2 9JT, UK

Abstract

The local segmental dynamics of anthracene labelled *cis*-1,4-polybutadiene in dilute solution and vinyl-1,2-polybutadiene in dilute solution have been studied by means of time-resolved optical spectroscopy as a function of temperature (298–323 K) and pressure (0.1–150 MPa) in several solvents (dioctyl phthalate, squalane, *cis*-decalin, *n*-dodecane and toluene) of good thermodynamic quality. This range of temperatures and pressures afforded a viscosity range of three decades. Kramers' theory predicts local motions that scale as the first power of the steady shear solvent viscosity. However, findings from this study reveal motions that scale as the 0.61 ± 0.03 power of the solvent viscosity for *cis*-1,4-polybutadiene and 0.75 ± 0.04 for vinyl-1,2-polybutadiene over the entire pressure and temperature range. © 2002 Published by Elsevier Science Ltd.

Keywords: Dilute solution; Segmental dynamics; Pressure

1. Introduction

Studies of local dynamics of polymer chains in solution afford valuable insight into the structure–property relationships of polymers. Motions at the microscopic level on the scale of a few repeat monomer units are sensitive to the chemical structure of those repeat units. Investigations into the solvent viscosity scaling of dilute solution local polymer dynamics have primarily been performed as a function of temperature in a variety of solvents [1–8]. Until recently [9], the role of pressure had not been investigated nearly as rigorously for these macromolecular motions. This is surprising due to the importance of pressure within polymer processing and polymer applications. This manuscript continues with the authors' previous study of the pressure dependence of the solution state local dynamics of *cis*-1,4-polyisoprene [9] through a study of the solution state local segmental dynamics of *cis*-1,4-polybutadiene (14PB) and vinyl-1,2-polybutadiene (12PB) via time-resolved optical spectroscopy (TROS). These 14PB and 12PB solution studies will also complement the authors' future efforts to monitor the pressure dependence of their melt local dynamics.

Measurements are performed as a function of temperature (298–323 K) and pressure (0.1–150 MPa) in several solvents affording a viscosity range of three decades. Kramers' theory in the high friction limit and in the absence of specific polymer/solvent interactions predicts a linear dependence of these dynamics on solvent viscosity. However, the motions are observed to scale as $\eta^{0.61\pm0.03}$ for 14PB and $\eta^{0.75\pm0.04}$ for 12PB over the entire pressure and temperature range employed. Scaling of local dynamics by a fractional power of the solvent viscosity is linked to the lack of separation in the timescales of the polymer and solvent dynamics as observed for flexible elastomers. Scaling of the local dynamics by solvent viscosity with exponents nearer to 1.0 is observed as this separation increases as observed for polystyrene with its bulky side group. A quantitative understanding of how the local dynamics of a given polymer scale with solvent viscosity is essential in any effort that is aimed at determining the correct inherent solution state activation energy of these macromolecular motions.

Section 2 summarises the experiment technique including the procedure to correct the data for pressure induced birefringence. Results including activation energies and activation volumes are presented and discussed in Section 3. A summary is found in Section 4.

* Corresponding author. Tel.: +44-113-3433812; fax: +44-113-3433846.

E-mail address: d.b.adolf@leeds.ac.uk (D.B. Adolf).

0032-3861/02/$ - see front matter © 2002 Published by Elsevier Science Ltd.
PII: S0032-3861(02)00549-9

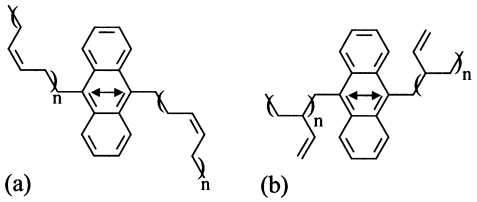

Fig. 1. Structure of anthracene-labelled *cis*-1,4-polybutadiene (a) and vinyl-1,2-polybutadiene (b). The $S_0 \rightarrow S_1$ transition is indicated by the double-headed arrow.

2. Experimental details

2.1. Materials and sample preparation

The anthracene centre labelled *cis*-1,4-polybutadiene (14PB) used in this study was purchased from Polymer Source, Inc., Canada. The labelled vinyl-1,2-polybutadiene (12PB) was purchased from Polymer Laboratories, UK. Each polymer chain contains one chromophore covalently bonded in the middle of the chain (Fig. 1). The $S_0 \rightarrow S_1$ electronic transition dipole moment of the chromophore is oriented along each chain backbone. Any movement of the dipole reflects movement of the polymer backbone. Physical characteristics are given in Table 1 along with molecular weight and polydispersity determined via size exclusion chromatography and microstructures found via ^{13}C NMR.

Dilute solutions of labelled polymer were prepared at polymer concentrations to give an optical density of ~0.1 in a 10 mm path length cuvette at 404 nm. To avoid fluorescence quenching each solution sample was subjected to at least three freeze-pump-thaw cycles to replace molecular oxygen with molecular nitrogen. The solvents employed were toluene (TOL), *n*-dodecane (DOD), *cis*-decalin (*cis*-decahydronaphthalene, DEC), squalane (SQU), and dioctyl phthalate (DPT) and all were used as received (Aldrich; all >99% purity). The viscosities of the solvents at ambient pressure (i.e. 0.1 MPa) are taken from literature [1,10,11]. High pressure viscosity data for these solvents were supplied by Dr N.F. Glen of the National Engineering Laboratory [12]. These data were generated using torsionally vibrating crystal viscometry [13], falling body viscometry [14], and rolling ball viscometry [15] and have an associated error of ±2%.

2.2. High pressure cell

The high pressure cell used in this study was purchased from ISS, Inc. Champaign, Illinois, USA. The cell consists of a drilled stainless steel alloy block with four window ports and a top plug for removal and replacement of samples. Measurements were performed using quartz windows with a diameter of 19 mm and a thickness of 8.5 mm. Two sets of window ports of different open aperture size were used to assess the extent to which aperture size affected the magnitude of the observed pressure-induced birefringence. The aperture sizes were 5 and 10 mm in diameter with the 5 mm aperture offering a greater support area for the optic. A significant reduction in the pressure induced birefringence is observed in Fig. 2 when the smaller diameter apertures are used (Section 2.5).

With the quartz windows, the cell can be pressurised up to 300 MPa with a maximum working temperature of 333 K. This manuscript reports data taken at temperatures of 298, 313 and 323 K and at pressures of 0.1, 50, 100, and 150 MPa at each of the three temperatures. Channels through the cell connected to an external bath allow temperature control to ±1 K. The pressurising medium is spectroscopic grade ethanol with the hydrostatic pressure generated by a hand pump.

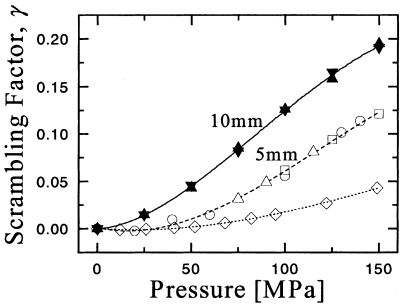

Fig. 2. Scrambling factors as a function of pressure. The closed triangles and the closed inverted triangles represent scrambling factors deduced from 14PB in DPT at 280 K and 14PB in TOL at 298 K, respectively, both using the 10 mm apertures. The open squares, open circles, and open triangles denote measurements of γ using 14PB in DPT at 280 K, 12PB in SQU at 280 K, and anthracene labelled *cis*-1,4-polyisoprene (14PI) in DPT at 280 K [9] all using the 5 mm apertures. Also shown are the correction factors found by Paladini and Weber [18] (open diamonds) for fluorescein in glycerol at 248 K. The solid curves running through each set of data are a best fit third degree polynomials with best fit parameters reported in Table 2.

2.3. Experimental technique

The TROS technique [16] and apparatus [17] have been described in detail elsewhere and only a brief description is

Table 1
Physical characteristics of the polymers used in this study

Polymer	$M_w \times 10^{-3}$	Polydispersity	Microstructure			
			% *cis*-1,4	% vinyl-1,2	% *trans*-1,4	Abr.
cis-1,4-PB	116.6	1.05	92	4	4	14PB
vinyl-1,2-PB	67.0	1.19	7	86	7	12PB

Table 2
Parameters of the third degree polynomial fit of the scrambling factor γ as a function of pressure P in MPa following $\gamma(P) = A_1P + A_2P^2 + A_3P^3$ for big and small aperture windows

Aperture (mm)	A_1 (MPa^{-1})	A_2 (MPa^{-2})	A_3 (MPa^{-3})
10	2.42×10^{-4}	1.63×10^{-5}	-6.22×10^{-8}
5	-2.04×10^{-4}	1.08×10^{-5}	-2.59×10^{-8}

given here. An anisotropic distribution of anthracene chromophores is photoselected using a short polarised pulse of light. Those chromophores with $S_0 \rightarrow S_1$ electronic transition dipole moments parallel to the excitation polarisation are preferentially excited. Since the excited state chromophores emit light directed along the transition dipole moment, fluorescence emission immediately after excitation is polarised. Within this study, the excitation wavelength is 404 nm for both 14PB and 12PB. The emission wavelength is 408 nm for 14PB and 414 nm for 12PB. A slight red shift of absorption and emission spectra with pressure (i.e. ~1.5 nm per 100 MPa) was observed.

Local segmental polymer dynamics are observed by monitoring the time-resolved decay of the polarisation of the emission fluorescence parallel, $I_{\|}(t)$, and perpendicular, $I_{\perp}(t)$, to the polarisation of the excitation pulse using time correlated single photon counting techniques.

A time dependent anisotropy function, $r(t)$, is calculated from these emission decays as

$$r(t) = \frac{I_{\|}(t) - I_{\perp}(t)}{I_{\|}(t) + 2I_{\perp}(t)}. \quad (1)$$

This is related to a second order orientational autocorrelation function, CF(t), as

$$r(t) = r_0 \mathrm{CF}(t) = r_0 \langle P_2(\cos\,\theta(t)) \rangle \quad (2)$$

through the fundamental anisotropy, r_0. P_2 is the second Legendre polynomial and $\theta(t)$ is the angle through which the transition dipole moment has rotated in time t since the excitation pulse.

2.4. Data fitting

An iterative impulse reconvolution process is used to deconvolve distortions in the data due to the finite width of the laser pulse (~5 ps) and the response of the detection equipment [16]. The anisotropy decays were then fit to the empirical biexponential function

$$r(t) = A \exp(-t/\tau_1) + B \exp(-t/\tau_2) \quad (3)$$

where A, B, τ_1, and τ_2 are fitting parameters. The biexponential fits are used only to characterise the shape of the anisotropy decays and no further significance is given to the fit parameters.

Reduced χ^2 values for these fits were typically ≤ 1.1. The overall timescale of the monitored segmental dynamic is determined via a correlation time, τ_c, of the decay defined as

$$\tau_c = \frac{1}{r_0} \int_0^{\infty} r(t)\mathrm{d}t. \quad (4)$$

Errors in the values of τ_c reported within this manuscript are ±10%. The value of r_0 for measurements at atmospheric pressure in this study was found to be 0.33 ± 0.02 in good agreement with values for other anthracene-labelled polymers found elsewhere [2,3].

2.5. Correction of pressure induced birefringence

The scrambling factor, γ, introduced by Paladini and Weber [18] is used to correct the experimental values of $I_{\|}(t)$ and $I_{\perp}(t)$ for pressure-induced birefringence of the quartz windows. γ is defined as

$$\gamma(P) = (1/3)[1 - (r_0(P)/r_0(P_{\mathrm{atm}}))] \quad (5)$$

where $r_0(P)$ and $r_0(P_{\mathrm{atm}})$ are the values of fundamental anisotropy at a pressure P and at atmospheric pressure, P_{atm}.

Fig. 2 presents scrambling factors for a variety of systems. The closed triangles and the closed inverted triangles represent scrambling factors deduced from 14PB in DPT at 280 K and 14PB in TOL at 298 K, respectively, both using the 10 mm apertures. The open squares, open circles, and open triangles denote measurements of γ using 14PB in DPT at 280 K, 12PB in SQU at 280 K, and anthracene labelled *cis*-1,4-polyisoprene (14PI) in DPT at 280 K [9] all using the 5 mm apertures. Similar data reported by Paladini and Weber [18] for fluorescein (open diamonds) in glycerol at 248 K are also shown for comparative purposes. All data for 14PB and 12PB presented within this work utilised the 5 mm window apertures. The curves running through each set of data are best-fit third degree polynomials with fit parameters reported in Table 2. The γ values used in this study are taken from these fits. The general shapes of these three curves are observed to be qualitatively similar. Quantitative differences are due to equipment specific factors such as the window material, thickness, mount geometry, and aperture size. The data also reveals a significant reduction in γ at high pressure when moving to the smaller apertures. Fig. 3 reveals excellent agreement between independent measurements of 14PB and 12PB local dynamics using either the 5 mm aperture or the 10 mm aperture. The value of r_0 for all data after correction was found to be 0.32 ± 0.02 averaged over all pressures and temperatures studied.

3. Results and discussion

To determine observed activation energies, the data were plotted in Arrhenius format. Examples of such plots, i.e. log τ_c versus 1000/T, at 0.1, 50, 100, and 150 MPa are given in Fig. 4 for 14PB and 12PB. The slope of each best-fit line

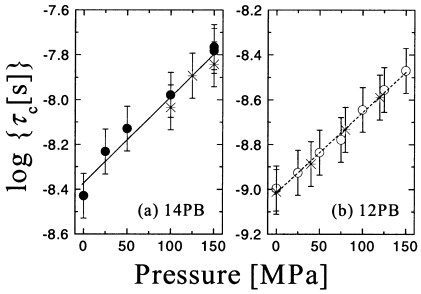

Fig. 3. Correlation times as a function of pressure for (a) 14PB in DPT at 323 K, and (b) 12PB in TOL at 298 K. Plots compares data obtained using the 5 mm window apertures (circles) to that using a second sample and 10 mm window apertures (asterisks). The solid and dashed lines are best fits to all the data.

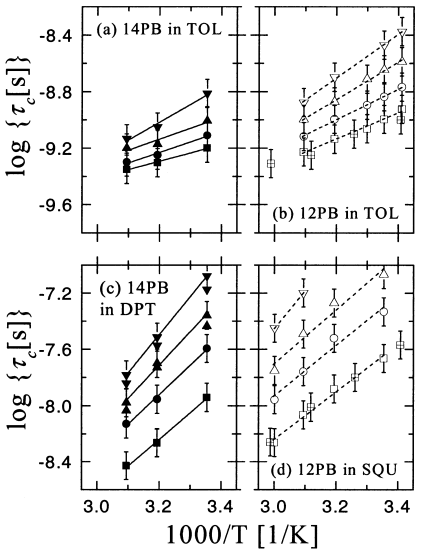

Fig. 4. Examples of correlation times for the dilute solution local dynamics of both anthracene labelled *cis*-1,4-polybutadiene (closed symbols) and vinyl-1,2-polybutadiene (open symbols) plotted in Arrhenius format. The plots show (a) 14PB in TOL, (b) 12PB in TOL, (c) 14PB in DPT, and (d) 12PB in SQU at 0.1 MPa (squares), 50 MPa (circles), 100 MPa (triangles), and 150 MPa (inverted triangles). Also shown as crossed squares on plots of 12PB dynamics are data from an earlier independent study at atmospheric pressure only [8]. Each line gives the experimentally observed activation energy E_{obs} for that solvent at that pressure.

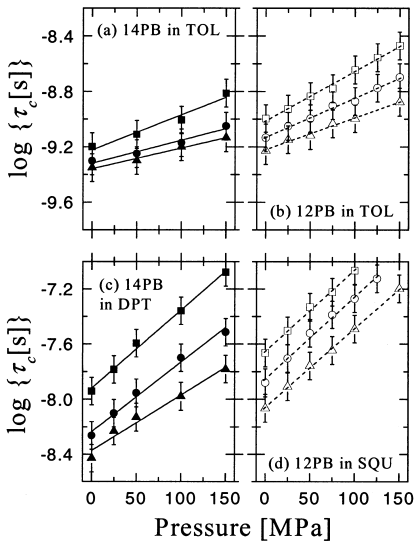

Fig. 5. Examples of correlation times for the dilute solution local segmental dynamics of anthracene labelled *cis*-1,4-polybutadiene (closed symbols) and vinyl-1,2-polybutadiene (open symbols) as a function of pressure. The plots show (a) 14PB in TOL, (b) 12PB in TOL, (c) 14PB in DPT, and (d) 12PB in SQU at 298 K (squares), 313 K (circles) and 323 K (triangles). Each line gives the experimentally observed activation volume V_{obs} for that solvent at that temperature.

running through the data affords the observed activation energy, E_{obs}, for local polymer dynamics within the indicated solvent at the indicated pressure. Values of E_{obs} for all solvents used are found within Table 3. For a given solvent, the local dynamics are slowest at low temperatures and high pressures. Fig. 5 reveals examples of plots of log τ_c versus pressure at 298, 313, and 323 K for 14PB and 12PB. Each best-fit line running through the data affords the observed activation volume, V_{obs}, for local polymer dynamics within the indicated solvent at the indicated temperature. Data taken at low pressure with minimal birefringence correction is in good agreement with high pressure data where the correction becomes larger. Values of V_{obs} for all solvents are found within Table 4.

Kramers' theory [19] predicts activated solution state dynamics within the high friction limit scale linearly with solvent viscosity as follows

$$\tau_c \sim \eta \exp(E_a/RT) \quad (6)$$

Table 3
The observed Arrhenius activation energies, E_{obs}, determined from the slopes of Fig. 4 as a function of pressure

Pressure (MPa)	E_{obs} for 14PB (kJ mol^{-1})				E_{obs} for 12PB (kJ mol^{-1})			
	TOL	DOD	DEC	DPT	TOL	DOD	DEC	SQU
0.1	11	17	26	36	17	19	19	32
50	14	17	27	40	21	25	22	39
100	15	18	30	45	25	27	25	42
150	24	20	33	52	30	29	28	–

There is an error of ± 10% associated with each value of E_{obs}.

Table 4
The observed activation volumes, V_{obs}, determined from the slopes of Fig. 5 as a function of temperature

Temperature (K)	V_{obs} for 14PB (cm^3 mol^{-1})				V_{obs} for 12PB (cm^3 mol^{-1})			
	TOL	DOD	DEC	DPT	TOL	DOD	DEC	SQU
298	14	20	19	32	20	21	25	34
313	10	18	18	30	17	21	22	36
323	9	16	15	25	14	17	20	35

There is an error of ± 10% associated with each value of V_{obs}.

Table 5
Values of the viscosity exponents α, activation energies E_a at atmospheric pressure and activation volumes V_a at 298 K for the dilute solution local dynamics of various elastomers showing the viscosity, pressure, and temperature range over which the values were obtained

Polymer	Method	α	E_a (kJ mol^{-1})	V_a (cm^3 mol^{-1})	Viscosity (mPa s)	Pressure (MPa)	Temperature (K)	Reference
14PB	TROS	0.61 ± 0.03	9.3 ± 1.5	2.5 ± 0.5	0.55–456	0.1–150	298–323	This work
	NMR[a]	0.33 ± 0.01	11.4 ± 1	–	0.23–41	0.1	306–328	[5]
	NMR[a]	0.34 ± 0.01	10.9 ± 1	–	0.23–41	0.1	306–328	[5]
12PB	TROS	0.75 ± 0.04	8 ± 2	2.8 ± 0.5	0.55–214	0.1–150	298–323	This work
	TROS	0.82 ± 0.04	8 ± 2	–	0.3–1500	0.1	280–350	[8]
	NMR[b]	0.43	14.1	–	0.3–3	0.1	315–415	[6]
14PI	TROS	0.65 ± 0.05	12 ± 1	1.6 ± 0.5	0.55–494	0.1–150	298–323	[9]
	TROS	0.75 ± 0.06	10 ± 1	–	0.4–320	0.1	270–340	[3]
	NMR[a]	0.41 ± 0.02	13 ± 2	–	0.3–30	0.1	250–360	[1]

[a] Refers to ^{13}C T_1 NMR measurements.
[b] Refers to ^{2}H T_1 NMR measurements.

where E_a is the intrinsic activation energy associated with the motion and R is the gas constant. For clarity, it is important to note that E_{obs} reflects contributions from E_a and the solvent's activation energy for viscous flow. Previous studies of elastomers utilising both TROS and T_1 NMR (i.e. ^{13}C and ^{2}H) at atmospheric pressure only have observed dynamics that scale by a fractional power of the viscosity and examples are shown in Table 5. In light of this, a modified form of Eq. (6) that is able to describe the solvent scaling of these motions as a function of temperature and pressure has been proposed as [20]

$$\tau_c \sim \eta^{\alpha} \exp[(E_a + PV_a)/RT] \quad (7)$$

where V_a is the intrinsic activation volume associated with the local dynamics. As with E_{obs} and E_a, V_{obs} reflects contributions from V_a and the solvent.

To determine E_a and V_a for the local segmental dynamics of 14PB and 12PB, a suitable value α is first found to allow contributions of the solvent to be properly accounted for. To determine the value of α, twelve plots of ln τ_c versus ln η at each studied temperature and pressure (i.e. three temperatures and four pressures) were generated for each microstructure. Examples of these plots are shown within Fig. 6.

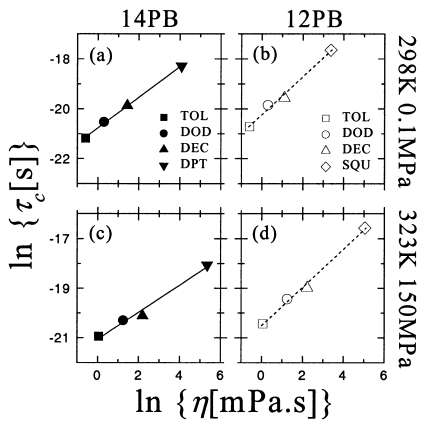

Fig. 6. Two of the twelve possible plots (see text) of ln τ_c as a function of ln η for each microstructure of polybutadiene. Each plot is generated from the values of τ_c for each of the solvents at a fixed temperature and pressure.

For 14PB values of α are observed to be 0.59, 0.61, 0.63, and 0.59 at the four studied pressures averaged over the three studied temperatures. Similarly, values of α are observed to be 0.62, 0.59 and 0.61 at the three studied temperatures averaged over the four studied pressures. An average value of α is 0.61 ± 0.03 over all available temperatures and pressures. Similarly for 12PB values of α are observed to be 0.77, 0.76, 0.74, and 0.71 at the four studied pressures and 0.73, 0.75 and 0.77 at the three studied temperatures. An average value of α is 0.75 ± 0.04 over all available temperatures and pressures.

The y-intercepts of the ln τ_c versus ln η plots are equal to $[E_a + PV_a]/RT$ at each temperature and pressure. V_a values are determined at each temperature by plotting the y-intercept of the ln τ_c versus ln η plots versus pressure at each temperature. Data for measurements at 298 K are shown within Fig. 7(a) (closed squares 14PB, open squares 12PB). The slope of each line is $[V_a/RT]$ at the indicated temperature. The value of V_a is temperature dependent in both cases (Table 6) with $V_a(T)$ decreasing with increasing temperature. The average value of V_a is 1.9 ± 0.5 cm^3 mol^{-1} for 14PB and 1.2 ± 0.5 cm^3 mol^{-1} for 12PB.

In order to calculate E_a, values of the y-intercept minus the contribution from $V_a(T)$ is plotted versus 1000/T at a

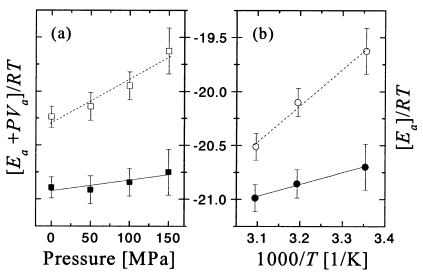

Fig. 7. y-Intercept data from the ln τ_c versus ln η plots plotted (a) against pressure and (b) against 1000/T. Plot (a) shows data for measurements at 298 K (closed squares 14PB, open squares 12PB). Plot (b) shows data for measurements at 150 MPa (closed circles 14PB, open circles 12PB).

Table 6
The Arrhenius activation energies, E_a, and activation volumes, V_a, determined from the slopes of Fig. 7 as a function of pressure and temperature, respectively

Polymer	E_a (kJ mol^{-1})					V_a (cm^3 mol^{-1})			
	0.1 MPa	50 MPa	100 MPa	150 MPa	Average	298 K	313 K	323 K	Average
14PB	9	9	10	9	9	2.5	2.2	1.0	1.9
12PB	8	14	14	–	–	2.8	0.8	0.0	1.2

There is an error of ± 10% associated with each value of E_a and of ± 20% for each value of V_a.

fixed pressure. This accounts for the temperature dependent activation volume. Examples of this data at 150 MPa are also shown within Fig. 7(b) (closed circles 14PB, open circles 12PB). Of the twelve possible ln τ_c versus ln η plots (i.e. Fig. 6) for 12PB, the two for 298 and 313 K at 150 MPa only contain data for TOL, DOD, and DEC (not shown). The time scales for the local motions of 12PB in SQU at these temperatures at 150 MPa were too slow to allow a reliable value of τ_c to be determined. Furthermore, these plots only cover a small viscosity range in comparison to the other plots and are therefore not used in any calculations of α, E_a, or V_a. The data for 14PB reveals a pressure independent E_a with an average value of 9 ± 1 kJ mol^{-1} (Table 6). The values of E_a for 12PB, however, show a dependence on pressure not seen for the 14PB data.

4. Summary

The local dynamics of anthracene labelled *cis*-1,4-polybutadiene and vinyl-1,2-polybutadiene in dilute solutions have been studied by means of TROS as a function of temperature (298–323 K) and pressure (0.1–150 MPa) in several solvents of good thermodynamic quality. Findings from this study reveal local motions scale as the 0.61 ± 0.03 power of the solvent viscosity for 14PB and as the 0.75 ± 0.04 power of the solvent viscosity for 12PB over the entire experimentally addressed pressure and temperature range as shown in Fig. 8. Quantitatively similar

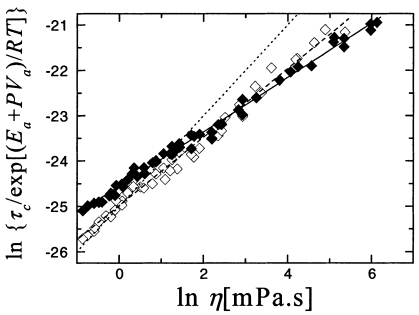

Fig. 8. A master plot showing data for all solvents at every temperature and pressure within this study with data for 14PB shown as closed squares, and data for 12PB shown as open squares. Values of E_a and V_a are as given in Table 6. The solid line is a fit to all the 14PB data and gives a value for α of 0.61 ± 0.03. The dashed line is a fit to all the 12PB data and gives a value for α of 0.75 ± 0.04. The dotted line represents Kramers' theory in the high friction limit (i.e. $\alpha = 1$).

behaviour is observed when the solvent viscosity is varied by pressure at fixed temperatures and by temperature at fixed pressures.

V_a values were found to be small relative to the measured V_{obs} values revealing V_{obs} is dominated by the contribution from the solvent. This finding in agreement with previous high pressure studies of small molecule isomerisation [21–23] and dilute solution 14PI segmental polymer dynamics [9]. However, in contrast to results for 14PI [9] activation volumes of both 14PB and 12PB found in this study appear to be temperature dependent within experimental error.

The activation energy of 14PB is found to be 9 ± 1 kJ mol^{-1} and independent of pressure within experimental error. Zhu et al. [5] determined a value of 11.4 ± 1 kJ mol^{-1} (CH-group) and 10.9 ± 1 kJ mol^{-1} (CH_2-group) for 14PB studied by ^{13}C T_1 NMR. The value of E_a for 12PB at atmospheric pressure was determined to be 8 ± 2 kJ mol^{-1} which compares well with the value of 8 ± 2 kJ mol^{-1} found by Adams and Adolf [8] also via TROS. Zhu and Ediger [6] report an activation energy of 13 ± 1 kJ mol^{-1} for 12PB via ^{2}H T_1 NMR. Larger E_a values from NMR studies of local polymer dynamics relative to values from TROS studies is consistent with similar work involving 14PI in dilute solution. The TROS measurements of Adolf et al. [3] afforded a value of 10 ± 1 kJ mol^{-1} whereas the ^{13}C T_1 NMR measurements of Glowinkowski et al. [1] revealed an activation energy of 13 ± 2 kJ mol^{-1}. It is interesting to note that 12PB demonstrates a pressure dependent activation energy not seen in 14PB or 14PI [9] observed over the same temperature and pressure range utilising similar solvents. One may wonder whether this is due to a pressure induced reduction in solvent quality as Waldow et al. [2,24] have reported atmospheric E_{obs} values of local polymer dynamics within θ solvents that are larger relative to their values within good solvents. However, such data would not collapse onto a single master curve as seen for 14PI and 12PI data in Fig. 8. Furthermore, high pressure viscosity measurements of dilute polymer solutions up to 2000 MPa due to Cook et al. [25] suggest chain characteristics within good solvents are not influenced by pressure. Additionally, the work of Imre and Van Hook [26] and Rebelo et al. [27] reveals pressure can improve solvent quality (i.e. non-solvent to a poor solvent and a poor solvent to a θ solvent). Further insight into the source of this pressure dependent

activation energy is hampered by the scarcity of high pressure studies of solution state polymer dynamics and the fact that many of the few existing studies do not report how pressure affects the observed activation energies. Current efforts are addressing whether this effect is observed in dilute solutions of polystyrene.

Acknowledgements

This work was supported through funding from EPSRC GR/R17232 and the IRC in Polymer Science and Technology within the Department of Physics and Astronomy at the University of Leeds, UK.

References

[1] Glowinkowski S, Gisser DJ, Ediger MD. Macromolecules 1990;23:3520.
[2] Waldow DA, Ediger MD, Yamaguchi Y, Matsushita Y, Noda I. Macromolecules 1991;24:3147.
[3] Adolf DB, Ediger MD, Kitano T, Ito K. Macromolecules 1992;25:867.
[4] Gisser DJ, Ediger MD. Macromolecules 1992;25:1284.
[5] Zhu W, Gisser DJ, Ediger MD. J Polym Sci, Polym Phys 1994;32:2251.
[6] Zhu W, Ediger MD. Macromolecules 1995;28:7549.
[7] Zhu W, Ediger MD. Macromolecules 1997;30:1205.
[8] Adams S, Adolf DB. Macromolecules 1998;31:5794.
[9] Punchard BJ, Adolf DB. Macromolecules 2002;35:3281.
[10] Viswanath DS, Natarajan G, Data book on the viscosity of liquids. New York: Hemisphere; 1989.
[11] Barlow AJ, Lamb J, Matheson AJ. Proc R Soc Lond A 1966;292:322.
[12] Glen NF. National Engineering Laboratory, East Kilbride, Glasgow G75 0QU, UK.
[13] Tanaka Y, Hosokawa H, Kubota H, Makita T. Int J Thermophys 1991;12:245.
[14] Dymond JH, Robertson J, Isdale JD. Int J Thermophys 1981;2:133.
[15] Krahn UG, Luft G. J Chem Engng Data 1994;39:670.
[16] O'Conner DV, Philips D, editors. Time-correlated single photon counting. New York: Academic Press; 1984.
[17] Adams S, Adolf DB. Macromolecules 1999;32:3136.
[18] Paladini AA, Weber G. Rev Sci Instrum 1981;52:419.
[19] Kramers HA. Physica 1940;7:284.
[20] Velsco SP, Waldeck DH, Fleming GR. J Chem Phys 1983;78:249.
[21] Hara K, Kiyotani H, Kajimoto OJ. Chem Phys 1995;103:5548.
[22] Hara K, Akimoto S, Susuki H. Chem Phys Lett 1990;175:493.
[23] Taniguchi Y, Senoo M, Hara K, editors. High-pressure liquids and solutions. Japan: The Society of Materials Science; 1994.
[24] Waldow DA, Johnson BS, Hyde PD, Ediger MD, Kitano T, Ito K. Macromolecules 1989;22:1345.
[25] Cook RL, King Jr. HE, Peiffer DG. Macromolecules 1992;25:2928.
[26] Imre A, Van Hook WA. J Polym Sci B: Polym Phys 1997;35:1251.
[27] Rebelo LPN, Visak ZP, Szydlowski J. Phys Chem, Chem Phys 2002;4:1046.